Virology 428 (2012) 11–20

Contents lists available at SciVerse ScienceDirect

Virology

journal homepage: www.elsevier.com/locate/yviro

Characterisation of simian immunodeficiency virus-infected cells in pigtail macaques

Wendy R. Winnall [1], Amy Sexton [1], Sheilajen Alcantara, Sarah Roath, Robert De Rose, Stephen J. Kent *

Department of Microbiology and Immunology, University of Melbourne, Royal Parade, Parkville, 3010 VIC, Australia

ARTICLE INFO

Article history:
Received 29 January 2012
Returned to author for revisions
12 March 2012
Accepted 24 March 2012
Available online 15 April 2012

Keywords:
SIV
CD3
CD4
$\alpha 4\beta 7$ integrin
Central memory T cells
p27

ABSTRACT

Defining which cells become infected with simian immunodeficiency virus (SIV) *in vivo* should assist in unravelling the pathogenesis of human immunodeficiency virus (HIV)/SIV infection. HIV/SIV infection of $CD4^+$ T cells resulted in down-regulation of CD3 and CD4 surface molecules *in vitro*, however this phenomenon is poorly characterised *in vivo*. Intracellular SIV p27 was studied by flow cytometry in serial blood samples and lymph node samples during acute infection of 17 SIVmac-infected pigtail macaques. Two weeks after infection, a mean of $56 \pm 6.8\%$ the $p27^+$ cells were lymphocytes negative for surface CD4 and CD3, and indeed the highest proportion of SIV infected cells were found in the small subset of $CD3^{Lo}CD4^-CD8^-$ lymphocytes, indicating that infection has lead to down-regulation of these markers *in vivo*. Furthermore, the relative amount of SIV p27 within lymphocytes (based of mean fluorescence intensity) was higher in $CD3^{Lo}CD4^-$ and $CD3^-$ infected cells than in $CD3^+$ or $CD4^+$ $p27^+$ populations, consistent with greater viral production in $CD4^+$ T cells down-regulating CD3 and CD4 molecules. The $CD3^-CD4^-$ infected cells expressed T cell markers CD2 and CD5 and were negative for monocyte, NK and B cell markers. The majority of infected cells were $CD28^+CD95^+$ central memory T cells. Surprisingly, $p27^+$ blood lymphocytes were mostly negative for activation markers CD25 and CD69, but most of the infected lymph nodes cells were activated. Our results characterise productively-infected macaque lymphocytes *in vivo*. The high proportion of SIV-infected lymphocytes that are $CD3^-CD4^-$ has important implications for the *in vivo* study of pathogenesis of SIV/HIV infections.

Introduction

A better understanding of how HIV spreads *in vivo* should ultimately lead to more refined strategies to treat or prevent infection. *In vitro* studies indicate that HIV or SIV infection of $CD4^+$ T cells results in down-regulation of CD4 from the cell surface, and that CD3 is also down-regulated by HIV-2 and most SIV strains (Aiken et al., 1994; Foster and Garcia, 2008; Levesque et al., 2004; Sanfridson et al., 1994; Schindler et al., 2006). Similarly MHCI and II, and CD28 are also down-regulated by HIV or SIV infection (Bell et al., 2001; Schwartz et al., 1996; Swigut et al., 2001). Although long-established *in vitro*, very few studies have addressed CD3 and CD4 down-regulation *in vivo*.

Lentiviral down-regulation of cell surface CD4 is best characterised in HIV-1-infected T cell lines. HIV-1 uses at least three mechanisms to reduce CD4 expression on the cell surface: the Nef accessory protein down-regulates surface CD4 by accelerating its endocytosis, the envelope gp160 precursor retains newly synthesised CD4 in the endoplasmic reticulum (ER) and the Vpu accessory protein induces degradation of CD4 complexed to Env-gp160 in the ER (Chen et al., 1996; Craig et al., 1998; Levesque et al., 2004; Martin and Nayak, 1996). The conservation of CD4 down-regulation across HIV and SIV species, as well as the multiple mechanisms involved, indicate the importance of CD4 down-regulation to HIV immunopathogenesis. Indeed, mutations in SIV or HIV-1 Nef which abrogate Nef's ability to down-regulate CD4 *in vitro*, lead to a significant reduction in viral load in infected subjects (Deacon et al., 1995; Iafrate et al., 2000).

Nef is also able to down-regulate CD3, along with the T cell receptor (TCR), from the cell surface *in vitro* (Schindler et al., 2006) but the mechanism by which this occurs is not as well characterised as that for CD4 down-regulation. Nef-mediated down-regulation of CD3, however, appears to have been lost in the lentiviral lineage that gave rise to HIV-1, but is maintained in most SIVs well as HIV-2 (Schindler et al., 2006). As for CD4, CD3 down-regulation is described *in vitro*, but *in vivo* evidence for this phenomenon is limited to two publications (Friedrich et al., 2010; Reynolds et al., 2010).

There is a body of evidence, primarily using PCR-based studies of sorted $CD4^+$ T cells, that HIV preferentially infects particular

* Corresponding author. Fax: +61 3 8344 3846.
E-mail addresses: wwinnall@unimelb.edu.au (W.R. Winnall), drcordle@yahoo.co.uk (A. Sexton), sal@unimelb.edu.au (S. Alcantara), sarahroath@gmail.com (S. Roath), r.derose@unimelb.edu.au (R. De Rose), skent@unimelb.edu.au (S.J. Kent).
[1] Denotes equal contribution of authors.

0042-6822/$ - see front matter © 2012 Elsevier Inc. All rights reserved.
http://dx.doi.org/10.1016/j.virol.2012.03.016

subsets of T cells *in vitro* and *in vivo*. These studies have shown that activated CD4 T cells, central memory CD4 T cells, and T cells expressing the $\alpha 4\beta 7$ integrin all support HIV infection or replication more efficiently that naïve T cells or $\alpha 4\beta 7^{-}$T cells (Brenchley et al., 2004; Cayota et al., 1993; Centlivre et al., 2011; Heeregrave et al., 2009; Kader et al., 2009; Schnittman et al., 1990). HIV infection is also detected in $CD4^{+}$ NK cells and in some $CD8^{+}$ T cells (Bernstein et al., 2009; Huete et al., 2001; Mercure et al., 1993). Defining the characteristics of infected cell populations *in vivo* based on $CD4^{+}$ T cell populations may be problematic when these cells down-regulate CD4 T cell expression, and infected cell populations with implications for immunopathogenesis may be overlooked.

Macaque SIV models permit knowledge of the timing of infection, and the pigtail macaque exhibits uniform and rapid progression to disease (Klatt et al., 2011). The sampling of blood at regular intervals during acute infection of macaques allows

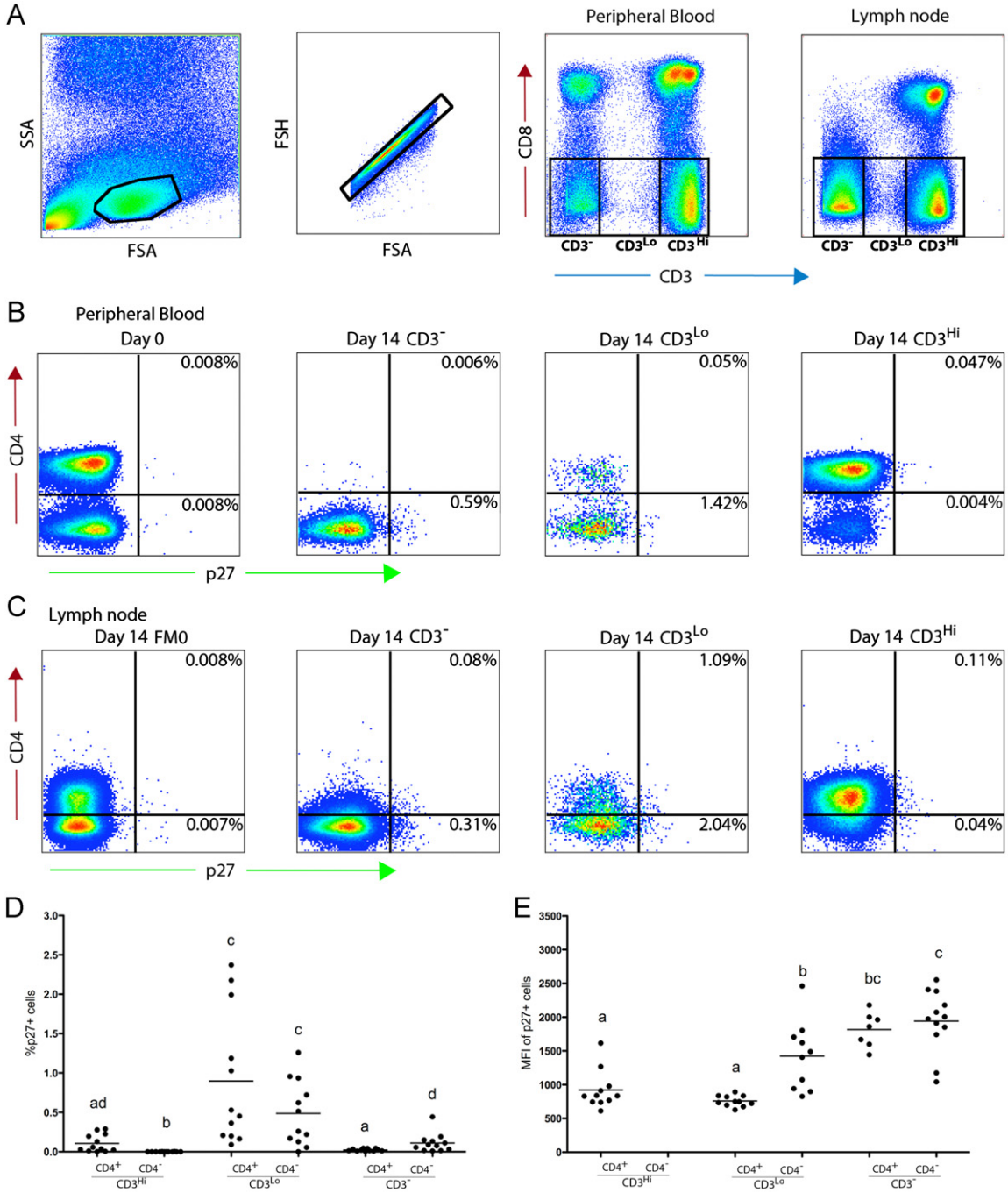

Fig. 1. Flow cytometric detection of SIV-infected ($p27^{+}$) peripheral blood and lymph node cells and comparison of infection in populations with differing levels of surface CD3 and CD4. (A) Peripheral blood and lymph node cell populations were gated for lymphocytes by forward (FSA) and side-scatter (SSA) properties (1st panel) and cell aggregates were excluded (2nd panel). The remaining cells were gated to select $CD8^{-}$ lymphocytes with $CD3^{-}$, $CD3^{Hi}$ and a small population for $CD3^{Lo}$ expression (3rd and 4th panels). The peripheral blood cells (B) and lymph node cells (C) within these gates were subdivided into $CD4^{+}$ and $CD4^{-}$ populations in which $p27^{+}$ was detected. The first panel shows the background from a control sample taken at day 0 for blood (population containing all $CD8^{-}$ lymphocytes) and a fluorescence minus one (FMO) for lymph nodes where anti-p27 was omitted from the staining mix. The remaining panels show $p27^{+}$ cells in the $CD3^{-}$, $CD3^{Lo}$ and $CD3^{Hi}$ populations. (D) The proportion of each of these populations of peripheral blood lymphocytes which were $p27^{+}$ at day 14 of infection over each infected animal. (E) The median fluorescence intensity (MFI) of p27 staining (where detected) for each of these populations at day 14 of infection. The number of animals in each group in (D) and (E) were all $n=12$.

a more detailed analysis of the *in vivo* infection of T cells than the study of HIV-infected individuals. Recent studies in SIV-infected rhesus macaques illustrated the loss of cell surface CD3 and CD4 molecules *in vivo*, in lymphocytes from lymph nodes after 19 weeks of infection (Friedrich et al., 2010; Reynolds et al., 2010). Herein, we characterise SIV-infected cells during acute SIVmac infection of 17 pigtail macaques. We show that a larger fraction of Gag expressing cells, and higher levels of viral antigens, are present in cell populations which had down-regulated CD3 and CD4 molecules.

Results

CD3 and CD4 down-regulation in SIV-infected lymphocytes in vivo

To assess the phenotype of SIV-infected cells *in vivo* we infected 17 pigtail macaques with SIVmac239 or SIVmac251 and studied serial blood and lymph node samples (day 14 only) by flow cytometry. Gated $CD8^-$ lymphocytes were divided into $CD4^+$ and $CD4^-$ populations and into $CD3^{Hi}$, $CD3^-$ and a small subset of $CD3^{Lo}$ cells lying between the $CD3^{Hi}$ and $CD3^-$ populations (Fig. 1A). Samples taken at day 0 as well as control samples with all antibodies except anti-p27 (FM0) were used to acurately gate on $p27^+$ cells (Fig. 1B and C). Two weeks after infection, small numbers of $CD3^{Hi}CD4^+$ cells expressing intracellular p27 were observed in both blood (Fig. 1B) and lymph node (Fig. 1C) preparations, with generally low fluorescent intensity of p27 expression; very few $CD3^{Hi}CD4^-$ cells were found to express p27. A mean of 56% ($n=11$, SEM 6.7%) of the $p27^+$ cells were negative for both CD3 and CD4 (data not shown). We found a significantly greater proportion of $p27^+$ cells in the $CD3^-CD4^-$ than the $CD3^{Hi}CD4^-$ population (Fig. 1D) ($F_{(5,59)}=31.42$, $p<0.001$). These $CD3^-$ p27-expressing cells also had significantly higher fluorescent intensity of p27 than the $p27^+CD3^{Hi}CD4^+$ population, suggesting higher amounts of p27 within these cells (Fig. 1E) ($F_{(4,46)}=27.73$, $p<0.001$). Across all the animals with $p27^+$ cells identified at day 14, we found the highest proportion of cells expressing p27 in the small $CD3^{Lo}$ populations (Fig. 1D).

Time course of $p27^+$ cells following acute infection

We studied the kinetics of p27 expression in peripheral blood cells over time. The peak of p27-expressing cells was 14 day after infection (Fig. 2A). The proportion of $p27^+$ cells 14 day after infection was significantly greater than 8, 17 or 22 days after infection (Friedman Test across all 7 time-points $\chi^2_{(6,\ n=13)}=43.543$ and Wilcoxon Signed Rank Tests as indicted in the figure). The peak in p27-expressing cells coincided with the peak in plasma viral RNA at or around this time (Fig. 2B). There was a rapid fall off in numbers of infected cells in the blood by 22 day after infection, when they were rarely detectable. Lymph node mononuclear cells had relatively high proportions of $p27^+$ cells 14 days after infection (mean=0.532%, range=2, Fig. 1.C) but fewer were detected 4 weeks after infection (0.285% in one animal, data not shown). There were no dramatic shifts in $p27^+$ cells between the different $CD3^{+/-}$ or $CD4^{+/-}$ populations over time, consistent with the rapid turnover of infected cells (data not shown).

$CD3^-CD4^-$ SIV-infected cells bear central memory T cell markers

Cells that express intracellular p27 but lack CD3 and CD4 markers could be clearly distinguished from lineages other than $CD4^+$ T cells. In fresh whole blood or thawed PBMC samples from a subset of SIV-infected animals we counter stained the $p27^+$ cells from blood and lymph nodes at day 14 with various cell surface

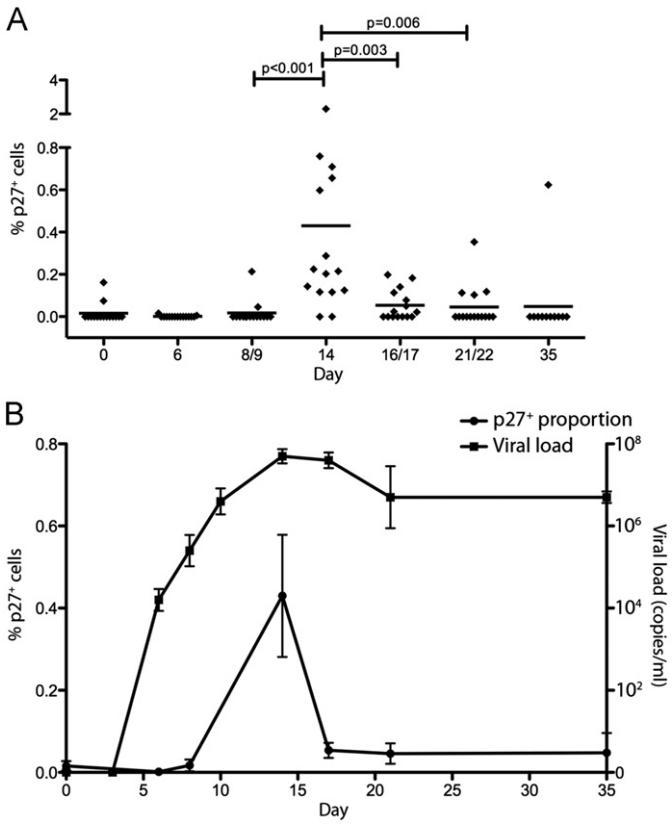

Fig. 2. Kinetics of p27 expression and viral load over time. (A) Comparison of the proportion of $p27^+$ among all $CD8^-$ lymphocytes from serial blood samples over the acute infection period. Statistical significance was determined using a Friedman test across all 7 time-points and individual comparisons were made using Wilcoxon Signed Rank tests. (B) Comparison of the mean proportion of $p27^+$ cells (left *y*-axis) with the viral load (right *y*-axis). Shown are mean and SEM for $n=12$ animals. Lines are a guide for the eye only.

markers. The $CD14^+$ (monocyte) populations were uniformly negative for $p27^+$ cells (Fig. 3A). The majority of the $p27^+$ cells stained positively for CD2 and CD5 (Fig. 3B–D), indicating that they were T cells. CD2 is also found on the surface of B cells and NK cells and CD5 is found on the surface of a subset of B-cells. We therefore demonstrated that the majority of infected $CD2^+$ cells were $CD20^-$ (92%, Fig. 3B), therefore unlikely to be B-cells, and negative for CD16 and CD56, which together identify NK cells and sub-populations of monocytes/granulocytes (Reeves et al., 2010) (80%, Fig. 3C). Furthermore, the infected $CD5^+$ cells were also $CD20^-$, indicating that they were not B-cells (67.8%, Fig. 3D).

Most actively and latently HIV-infected CD4 T cell populations identified by PCR techniques are central memory T cells (Brenchley et al., 2004). In the macaque, these central memory cells bear the surface markers CD28 and CD95 (Pitcher et al., 2002). Notably, the loss of $CD28^+CD95^+$ central memory CD4 T cells predicts progression to AIDS in SIV-infected rhesus macaques (Letvin et al., 2006). We therefore counter-stained macaque blood and lymph node samples from the acute SIV infection period (days 9 to 22 and day 14 only for lymph nodes) with CD3/4/8/28/95 surface markers and intracellular p27 to determine the proportion of central memory T cells among the infected population. CD8 staining was used to exclude $CD8^+$ T cells form these analyses. A median of 35.8% (range: 18% to 46% over 5 time-points) of peripheral blood and 47% of lymph node $CD4^+$ T cells (Day 14 only) were $CD28^+CD95^+$ central memory T cells (Fig. 4A and B, first column). In contrast, a median of 66.7% (range: 38–72%) of the peripheral blood $p27^+$ cells were $CD28^+CD95^+$ and median of 77% (range: 69–84%) of infected lymph node lymphocytes were $CD28^+CD95^+$

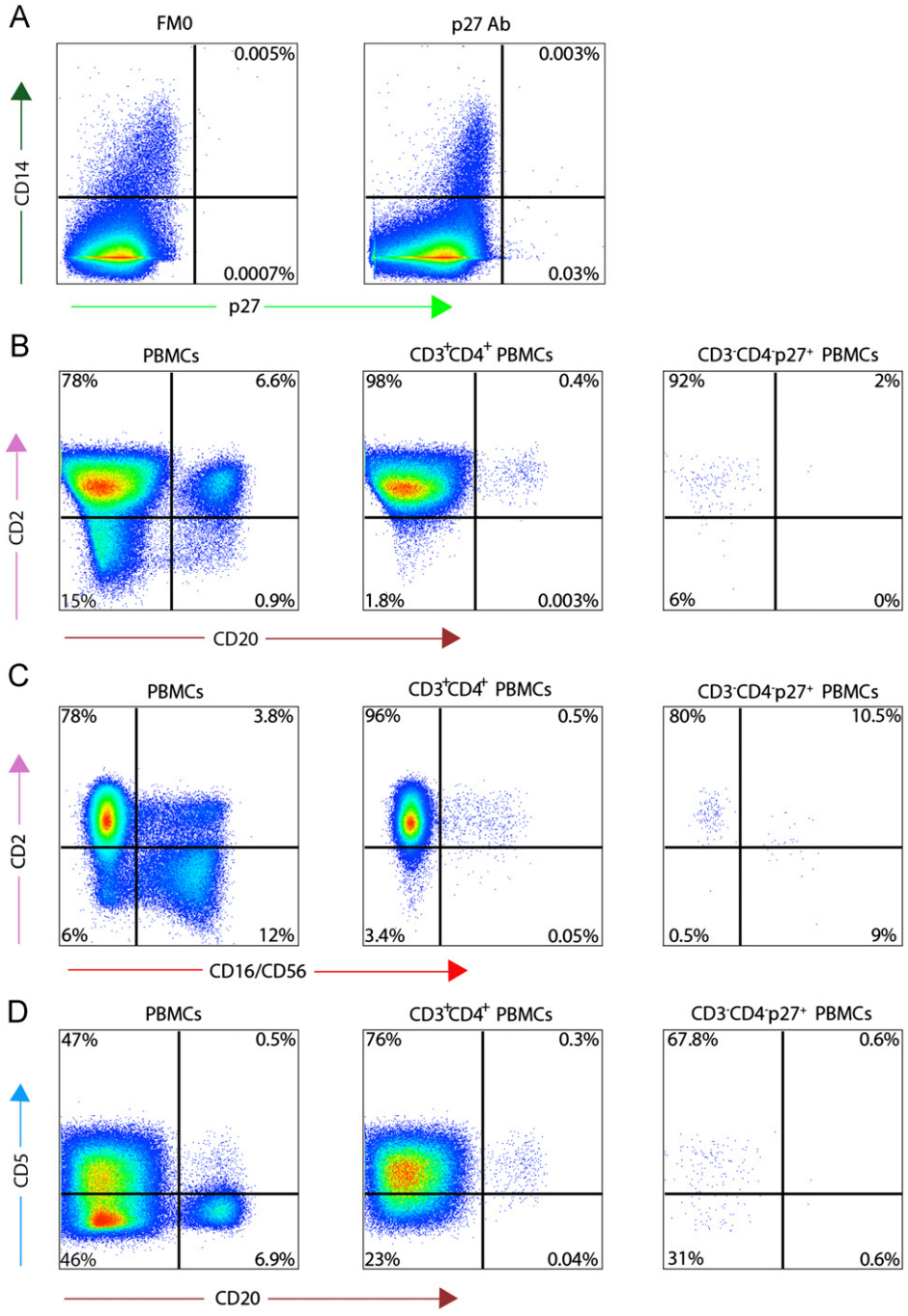

Fig. 3. The $CD3^{-}CD4^{-}$ infected cells express surface T cell markers but not markers for monocytes, B lymphocytes or NK cells. (A) Comparison of CD14 surface expression on $CD8^{-}$ peripheral blood cells which were either $p27^{+}$ and $p27^{-}$. The left panel is a fluorescence minus one control (FM0) where only anti-p27 was omitted, showing some non-specific fluorescence from CD14 positive cells (top right quadrant). The right panel shows p27-labelled cells in the $CD14^{-}$ quadrant only (bottom right quadrant). Analysis of CD2 *versus* CD20 labelling (B), CD2 *versus* CD16a/CD56 labelling (C) and CD5 *versus* CD20 labelling (D) of thawed PBMCs from day 14 of infection. For each row, the populations in the left panels are all live PBMCs, used to set the gates, in the middle panel are $CD3^{+}CD4^{+}$ T cells and in the right panel are $p27^{+}$ PBMCs. Results are representative of the 2 animals examined.

(Fig. 4A and B second column). These results indicate that central memory T cells were over represented in the infected cell population. Also apparent were a corresponding decrease in the proportion of the $CD28^{+}CD95^{-}$ naïve T cells (from median of 58% to 9.5%) and possibly a small increase in the proportion of $CD28^{-}CD95^{+}$ effector T cells (from median of 9.6%–24%) among the infected population compared to the total $CD4^{+}$ T cells population. When $CD3^{-}CD4^{-}$ infected cells (third column) were compared to $CD3^{+}CD4^{+}$ infected cells (fourth column), the double negative population was more likely to be $CD28^{-}$ than double positive infected cells, identifying them as effector memory T cells. However, infection can also lead to down-regulation of CD28, making this change in CD28 expression difficult to interpret (Bell et al., 2001).

Mucosal homing integrin (α4β7) and activation markers expressed by SIV-infected cells

The ability to individually detect SIV-infected cells by flow cytometry allows us to further phenotype these cells for mucosal homing integrins and activation markers. The mucosal homing

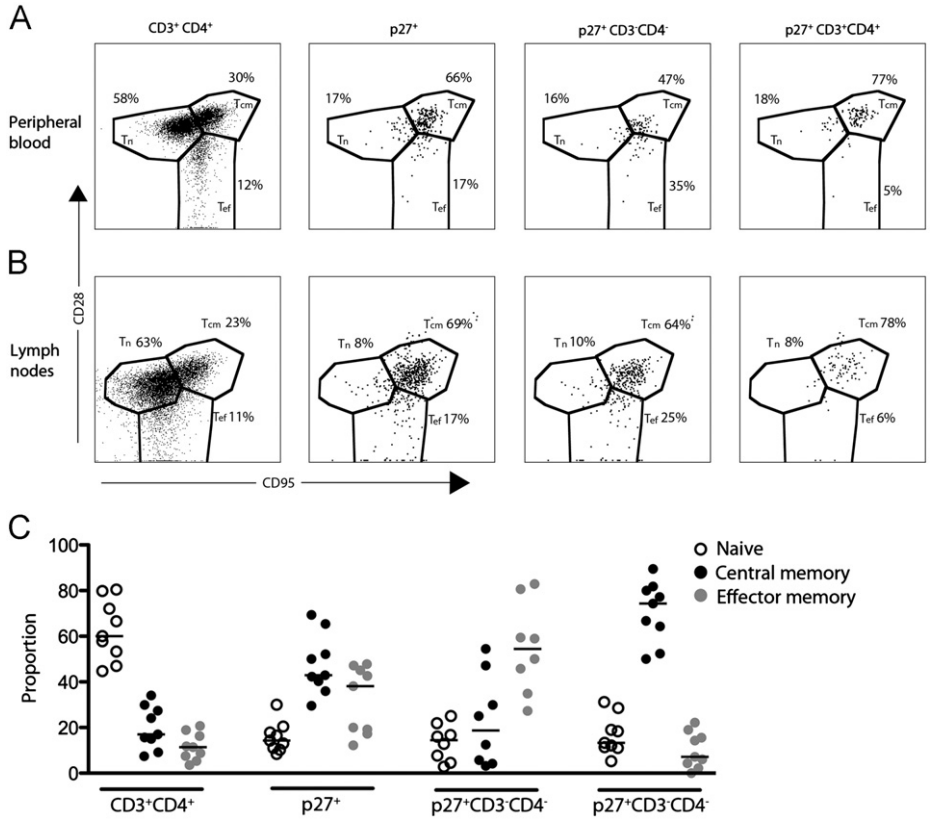

Fig. 4. Infected peripheral blood and lymph node cells express central memory T cell markers. CD28 and CD95 expression on $CD8^-$ peripheral blood lymphocytes (A) and lymph node cells (B) on day 14. In each row, the populations in the first panel are $CD3^+CD4^+$ lymphocytes used to set the gates. In the 2nd panel the populations are $p27^+CD8^-$ lymphocytes. The populations in the next two panels are $p27^+$ lymphocytes which were $CD3^-CD4^-$ and $CD3^+CD4^+$ as indicated. Tn refers to naïve, Tcm to central memory and Tef to effector memory T cells. (C) The proportions of naïve T cells (white circles), central memory T cells (black circles) or effector memory T cells (grey circles) among $CD8^-$ lymphocytes populations: $CD3^+CD4^+$, $p27^+$, $p27^+CD3^-CD4^-$ and $p27^+CD3^+CD4^+$ as indicated under the *x*-axis. Two animals over 4 to 5 time-points are shown which indicates a trend, but no statistics could be done to analyse these data. Lines depict medians for each group.

integrin $\alpha4\beta7$ allows T cells to track to mucosal sites such as the gut (Kilshaw and Murant, 1991). When we co-stained peripheral blood for both p27 and $\beta7$ at day 14 of SIV infection we found that, although the $\beta7^{Hi}$ population was somewhat enriched for $p27^+$ cells, the majority of the infected cells were $\beta7^{Lo}$ or negative (Fig. 5A). These results were consistent over 2 animals and 5 time-points (9–22 day post infection) (Fig. 5B). Within the lymph node cells few $\beta7$ positive cells were detected, as expected, since they do not migrate to this region in substantial numbers (data not shown). The proportions of $\beta7$-high or low populations among infected cells did not differ greatly when $CD3^-CD4^-$ infected cells were compared to $CD3^+CD4^+$ infected cells (data not shown).

Activated $CD4^+$ T cells are ready targets for productive HIV/SIV infection and *in vitro* experiments show higher levels of productive infection are achieved in activated compared to unactivated $CD4^+$ T cells (McDougal et al., 1985; Nabel and Baltimore, 1987). We studied the surface activation markers CD25 and CD69 in $p27^+$ cells and in $p27^-$ $CD3^+CD4^+$ lymphocytes in blood (9–22 day post infection) and lymph nodes 14 day after SIV infection. Peripheral blood contained only a small proportion of $CD25^+/CD69^+$ CD4 T lymphocytes (usually less than 10%) and the proportions of $p27^+$ cells that expressed activation markers were consistently similar to the $p27^-$ cells over 2 animals and 5 time-points (Fig. 5C and E). However, in lymph node mononuclear cells, the overall levels of activated lymphocytes were higher than in the blood (~25%) and the $p27^+$ cells were highly enriched for expression of the activation markers (~75%) (Fig. 5D and F). The proportions of activated infected cells did not differ greatly when $CD3^-CD4^-$ infected cells were compared to $CD3^+CD4^+$ infected cells (data not shown).

SIV infection of $CD8^+$ T cells

CD4 is generally regarded as an essential primary receptor for HIV/SIV infection of cells, although there have been older reports of HIV infection of peripheral blood CD8 T cells (Livingstone et al., 1996). Since small populations of $CD4^+CD8^+$ lymphocytes circulate, we analysed whether we could detect p27 expression in $CD8^+$ lymphocyte fractions 14 day after infection. We gated on $CD8^+$ lymphocytes and analysed cells for CD3 and CD4 expression as well as p27 expression (Fig. 6A). In 12 of the animals studied we detected low level but definite p27 expression in $CD8^+$ lymphocyte fractions (Fig. 6A and B). The proportions of $p27^+$ expression in $CD8^+$ lymphocytes were consistently less than those observed in $CD8^-$ lymphocytes. Interestingly, the pattern of infection was similar to the $CD8^-$ fraction studied above, *i.e.* the highest proportion of infected cells was detected in the $CD4^-CD3^-$ T cells, however the differences between these proportions were not statistically significantly (Kruskal Wallis test: $\chi^2_{(3,\ n=48)}=6.11$, $p=0.106$). These data suggest that SIV is able to infect $CD4^+CD8^+$ double positive T cells resulting in down-regulation of CD4 and CD3, as for $CD4^+CD8^-$ T cells.

Discussion

The precise identification of SIV-infected cell populations has important implications for HIV and SIV pathogenesis studies. Many previous studies detecting SIV/HIV-infected cells *in vivo* start with the assumption that $CD3^+CD4^+$ T cells are the primary

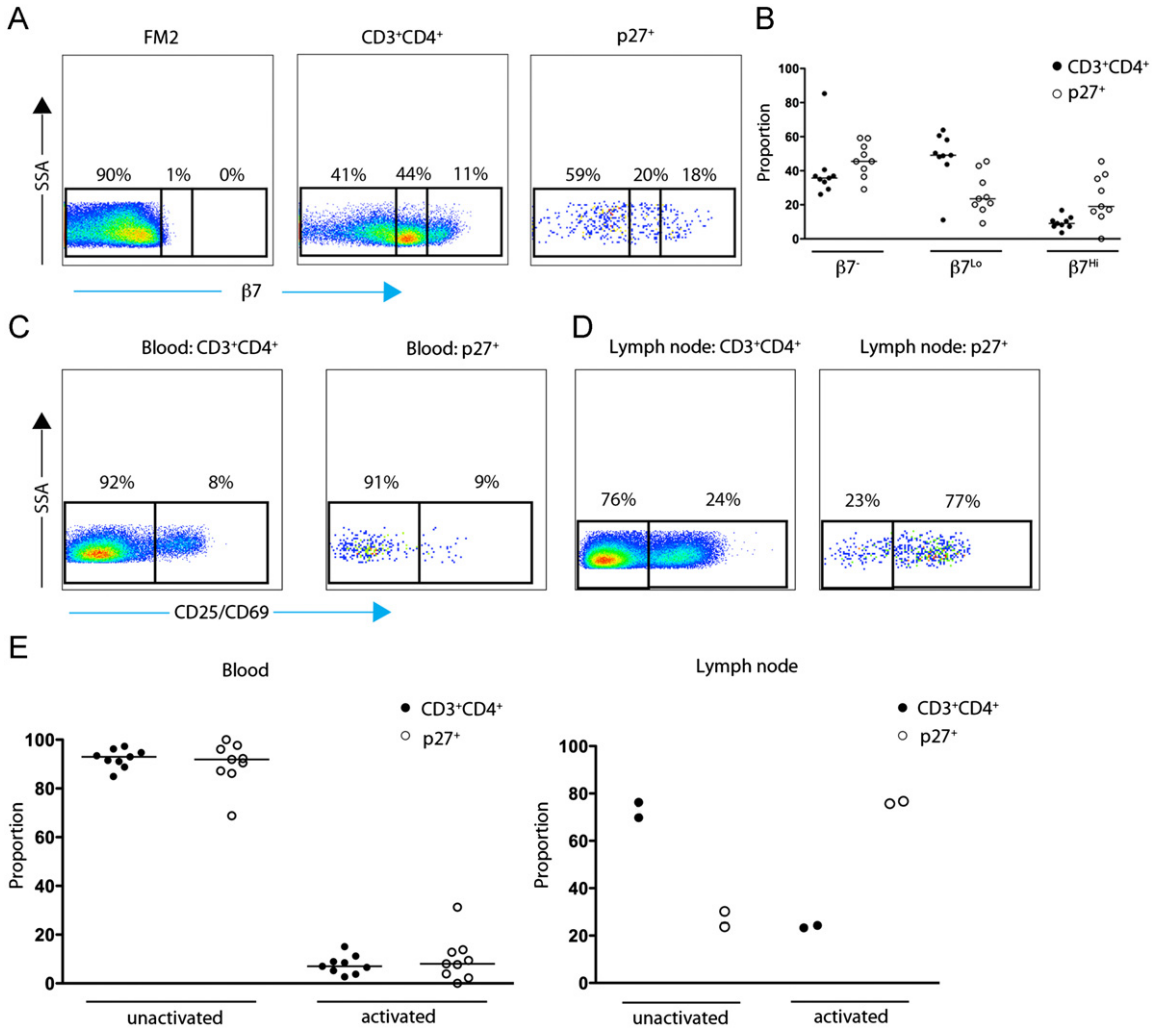

Fig. 5. Mucosal homing integrin ($\beta7$) and activation marker expression by infected peripheral blood and lymph node cells on day 14. (A) Gating strategy to detect $\beta7$ expression compared to side scatter properties (SSA) in a "fluorescence minus 2" control (FM2) where anti-p27 and anti-$\beta7$ were omitted (left hand panel), in $CD3^+CD4^+$ lymphocytes (middle panel) and in $CD8^-p27^+$ lymphocytes (right panel). Gates were designed to detect $\beta7^-$, $\beta7^{Lo}$ and $\beta7^{Hi}$ cells. (B) The proportions of $CD3^+CD4^+$ lymphocytes (black circles) and $CD8^-p27^+$ lymphocytes (white circles) which were $\beta7^-$, $\beta7^{Lo}$ or $\beta7^{Hi}$ cells. Two animals over 4 to 5 time-points are shown which indicates a trend, but no statistics could be done to analyse these data. Lines depict medians for each group. (C and D) Gating strategy to detect activated ($CD25^+$ and/or $CD69^+$) cells among peripheral blood lymphocytes (C) and lymph node cells (D). Expression of CD25/CD69 compared to side scatter properties (SSA) in $CD3^+CD4^+$ lymphocytes (left panel) and in $CD8^-p27^+$ peripheral blood lymphocytes (right panel). (D) Expression of CD25/CD69 in the same populations of lymph node cells. (E) The proportions of $CD3^+CD4^+$ lymphocytes (black circles) and $CD8^-p27^+$ lymphocytes (white circles) which were unactivated ($CD25^-CD69^-$) or activated ($CD25^+$ and/or $CD69^+$) cells. Two animals over 4 to 5 time-points are shown which indicates a trend, but no statistics could be done to analyse these data. Lines depict medians for each group. Results are representative of 2 animals over 4 time-points examined. (F) The proportions of $CD3^+CD4^+$ lymph node cells and $CD8^-p27^+$ lymph node cells which were unactivated or activated cells in two animals at one time-point (14 day after infection).

target for infection (Brenchley et al., 2004; Cayota et al., 1993; Centlivre et al., 2011; Heeregrave et al., 2009; Mattapallil et al., 2005). In the present study, intracellular staining of peripheral blood and lymph node cells for the SIV capsid protein p27 identified productively-infected cells, of which approximately half lacked surface CD3 and CD4. Although it is likely true that $CD3^+CD4^+$ T cells are the primary lymphocyte targets of SIV infection, our studies actually indicate that a large proportion of infected cells *in vivo* had down-regulated surface CD4 and CD3. That these infected $CD3^-CD4^-$ cells were once T cells is supported by the detection of other T cell markers on their cell surface (CD2 and CD5) and the absence of other lineage markers: CD14 which identifies monocytes, CD20 which identifies B cells, and CD56/CD16a which together identify NK cells in macaques, as well as some $CD56^+$ monocytes and $CD16^+$ granulocytes (Reeves et al., 2010). It is important to note that latently-infected cells would not be part of the infected population characterised in our study, and that some $CD4^+$ cells which stain positively for p27 may have virus attached to cell surface CD4 but not internalised.

The apparent loss of surface CD3 and CD4 from SIV-infected cells indicates that infection has lead to down-regulation of these proteins from the cell surface, however we have not formally demonstrated down-regulation events *in vivo*. During experiments where this was attempted, we discovered a considerable amount of intracellular expression of these markers in cells with concomitant surface staining. This obscured any increase in intracellular levels in infected cells following removal of these proteins from the cell surface (data not shown). Down-regulation of CD3 and CD4 by SIV infection is consistent with numerous studies in cultured HIV or SIV-infected cells (Aiken et al., 1994; Foster and Garcia, 2008; Levesque et al., 2004; Sanfridson et al., 1994; Schindler et al., 2006), two similar macaque experiments (Friedrich et al., 2010; Reynolds et al., 2010) but not with an earlier study (Schnittman et al., 1989). One study reported that

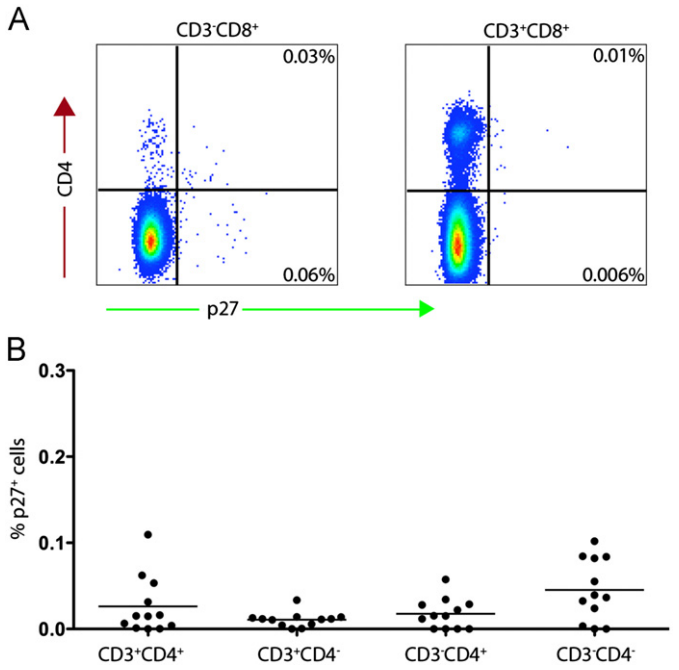

Fig. 6. Flow cytometric detection of p27$^+$ cells in the peripheral blood CD8$^+$ lymphocyte population. (A) CD8$^+$ peripheral blood lymphocytes were divided into CD3$^-$ and CD3$^+$ populations (gating strategy not shown). Staining for p27 and CD4 was compared in the CD3$^-$CD8$^+$ lymphocyte population (left panel) and CD3$^+$CD8$^+$ lymphocyte population (right panel). (B) The proportion of each of these populations of CD8$^+$ lymphocytes which were p27$^+$ at day 14 of infection over each of the 12 animals which had infected CD8$^+$cells.

90% of SIV-infected lamina propria cells were CD4$^+$ cells, but these immunohistochemistry results demonstrated CD4 protein expression which may have been on the surface or intracellular (Li et al., 2005). We propose that, at least initially, these markers would first be removed from the cell surface then degraded, based on cell culture experiments (Foster and Garcia, 2008; Greenberg et al., 1997; Sanfridson et al., 1994). However, it was interesting to note that the highest proportion of SIV-infected cells was in the populations with low expression of surface CD3; cells which are likely to be in the process of down-regulating this molecule. Furthermore, higher levels of the p27 protein (measured by higher MFI, Fig. 1E) were detected within infected cells with no surface CD3 and CD4. Staining of CD4 with a brighter fluorochrome might reveal low levels of surface CD4, indeed Reynolds (2010) found that a CD4^{Lo} population were also p27$^+$ using a brighter conjugate of CD4. We speculate that the CD3$^-$CD4$^-$ population of cells had been infected for a longer period of time, allowing time for both down-regulation of these molecules and higher levels of viral antigen expression.

The biological relevance of CD3 and CD4 down-regulation events has not been determined, but there are many suggested reasons for this phenomenon. CD4 down-regulation from the surface is suggested to aid release of the virus by diminishing the ability of CD4 to bind to gp120 on the budding virion, to stop CD4 being incorporated into the virion membrane and to reduce the possibility of multiple infections which might kill the cell too rapidly (Das and Jameel, 2005; Levesque et al., 2004). Interestingly, the extent of CD3 down-regulation *in vitro* by differing *Nef* alleles inversely correlated with the severity of SIV infection of sooty mangabeys, indicating that CD3 down-regulation was beneficial to the host (Schindler et al., 2008). CD3 down-regulation was proposed to prevent activation-induced cell death in this model. The present study does not support a benefit to the host of CD3 down-regulation, since considerable loss of surface CD3 was detected in the pigtail macaque model in which progression to AIDS is relatively rapid (Klatt et al., 2011). At least in the lymph nodes, considerable activation of CD3$^-$ infected cells indicates minimal resistance of SIV-infected lymphocytes to activation in our model.

Most of the CD3$^-$CD4$^-$ infected cells expressed CD2 and CD5 indicating that they were once T cells. Further evidence of their identity comes from CD28 expression (expressed on naïve and central memory T cells), as well as a lack of markers for monocytes, NK cells and B-cells. Interestingly a very small proportion of cells were positive for CD16/CD56, indicating that they could be infected NK cells, consistent with *in vitro* studies where HIV could infect CD4$^+$ NK cells in culture, leading to CD4 down-regulation (Bernstein et al., 2009). We also detected small populations of CD8$^+$ lymphocytes that had intracellular p27 expression, consistent with some previous studies (Flamand et al., 1998; Huete et al., 2001; Marodon et al., 1999). These cells were generally either CD8$^+$CD4$^+$ double positive cells or had a pattern of CD4 and CD3 down-regulation very similar to that observed in the CD8$^-$ population. These results are consistent with the hypothesis that CD8$^+$CD4$^+$ double positive T cells can be infected with SIV *in vivo* and that, as for CD4$^+$ T cells, the infection results in down-regulation of CD3 and CD4. A previous study characterising double positive cells from rhesus macaques blood showed them to be mostly central memory cells (CD28$^+$CD95$^+$) with similar levels of activation to blood CD4$^+$ T cells (approximately 20% CD25$^+$CD69$^+$) (Pahar et al., 2006). It is interesting to note that double positive T cells are abundant in the intestinal lamina propria of rhesus macaques. These intestinal double CD4$^+$CD8$^+$ T cells have a memory phenotype, are highly activated and express high levels of the HIV/SIV co-receptor CCR5 (Pahar et al., 2006), which we predict would make them a prime target for productive infection in the gut.

The ability to define SIV infected cells *in vivo* allowed us to study several aspects of the preferred targets of SIV infection. Our experiments confirm the high specificity of SIV for CD28$^+$CD95$^+$ central memory T cells (Brenchley et al., 2004; Heeregrave et al., 2009; Schnittman et al., 1990; Willerford et al., 1990). Interestingly, CD28$^-$CD95$^+$ cells were more likely to be infected from the CD3$^-$CD4$^-$ infected population than the CD3$^+$CD4$^+$ infected population, indicating that effector memory T cells were over-represented among infected cells with down-regulated CD3 and CD4. However, HIV and SIV are also known to down-regulate surface CD28 (Bell et al., 2001; Swigut et al., 2001), at least *in vitro*. Therefore the true identity of these CD3$^-$CD4$^-$ infected cells that are CD28$^-$CD95$^+$ cells requires further investigation.

It has been widely predicted that HIV and SIV-infected cells are more likely to be activated since these viruses replicate more efficiently in activated cells *in vitro* (McDougal et al., 1985; Nabel and Baltimore, 1987). Interestingly, we did not detect higher levels of productively-infected cells in the CD25$^+$/CD69$^+$ (activated) blood lymphocyte population, with the vast majority of p27$^+$ cells lying within the unactivated cells. However we found higher levels of infected cells in activated, compared to unactivated lymph node lymphocytes, consistent with preferential HIV-1 infection of activated CD4$^+$ T cells in lymph nodes (Meditz et al., 2011). The study of other activation markers such as HLA-DR, CD38 and Ki67 might be useful to fully characterise activation of infected cells in future studies.

Mucosal homing T cells are important in HIV/SIV pathogenesis both since they are rapidly depleted during HIV/SIV infection (Arthos et al., 2008; Kader et al., 2009) and due to their role in mucosal immunity (Czerkinsky and Holmgren, 1994). The mucosal homing integrin $\alpha4\beta7$ may act as a co-receptor for HIV infection allowing preferential targeting of $\alpha4\beta7$-expressing cells by HIV/SIV infection (Cicala et al., 2009). In previous studies, the

depletion of $\alpha4\beta7$-high expressing peripheral CD4 T cells correlated with the depletion of gut CD4 T cells in SIV infection (Kader et al., 2009). We were not able to confirm high level targeting of $\alpha4\beta7$-expressing lymphocytes *in vivo*. Although the $\beta7$-high expressing blood lymphocytes were modestly enriched for $p27^+$ cells, the majority of infected cells were in $\beta7^{Lo}$ or $\beta7^-$ cells. It is possible that the $\alpha4\beta7$-high expressing blood lymphocytes rapidly die after infection and cannot be visualised, however our studies were conducted during acute infection and other $p27^+$ populations were readily detectable. Of course, a different picture may be observed in future studies of gut mucosal lymphocytes.

The flow-based p27 Gag protein assay detects viral proteins and as there are no other viral protein assays that can be performed on a per cell basis, it is difficult to assess the sensitivity of the assay directly. It is likely that the substantial level of binding required to detect p27 protein contributes to the detection rate of ~0.4% of T cells being $p27^+$ during acute infection found by both us and other groups that have used the same assay (Friedrich et al., 2010; Reynolds et al., 2010). Thus we predict that this flow assay for $p27^+$ cells detects cells with highly productive infection. This is consistent with our finding that infected cells undergoing CD3 and CD4 down-regulation have higher fluorescent intensity of p27 staining. PCR based assays to detect viral DNA or RNA are likely to be more sensitive (detecting single copies) but do not assess whether the nucleic acids actually lead to highly efficient protein production. For example, Mattapillil (2005) showed, by sorting small numbers of $CD4^+$ T lymphocytes from macaques during acute SIV infection, that 30–60% of all $CD4^+$ T cells contained Gag DNA. However, on average the cells contained only 1.5 copies of SIV DNA per cell across both PBMC and lymph node cells suggesting that most cells do not have highly productive infections even though viral nucleic acids can be detected.

In summary, down-regulation of both CD3 and CD4 molecules appears to be common in SIV-infected cells *in vivo*, such that a high proportion of productively-infected cells in both blood and lymph nodes do not initially appear to be $CD3^+CD4^+$ T cells. It will be of interest to repeat our findings in humans with acute HIV infection, but this work provides a cautionary note to researchers only studying CD4 and CD3-expressing cells for HIV/SIV infection.

Materials and methods

Macaques and SIV infections

Seventeen pigtail macaques (*Macaca nemestrina*) were sourced from the Australian National Macaque Breeding Facility that were free from simian retrovirus D and tuberculosis and had not been previously infected with SIV. Fifteen macaques were infected with SIVmac251 10^4 TCID50 intravaginally via atraumatic instillation as previously described (Kent et al., 2005) and two with 600 μg of SIVmac239 proviral DNA IM as previously described (Kent et al., 2001; Loh et al., 2008). Animals were sedated with Ketamine during all procedures, including the serial blood and lymph node biopsies. The relevant institutional animal ethics committees approved all studies.

Antibodies

Anti p27-FITC (clone 55-2F12; NIH AIDS Research and Reference Reagent Programme) was kindly provided by Dr Nancy Wilson, University of Wisconsin (Friedrich et al., 2010). Antibodies to phenotype infected cells were raised to: CD2 Per-CPCy5.5 (BD (San Jose, *CA*), clone RPA-2.10, cat. 560643), CD3 Pacific blue (BD, clone SP34-2, cat. 558124), CD3 AF700 (BD, clone, SP32-4, cat. 557917), CD4 AF700 (BD, clone L200, cat. 560836), CD4 V450 (BD, clone L200, cat. 550811), CD4 PerCP (BD, clone L200, cat. 550631), CD5 APC (Invitrogen, Carlsbad, *CA* clone 5D7, cat. MHCD0505), CD8 Pe-Cy7 (BD, clone SK1, cat. 335787), CD8 Pac blue (BD, clone RPA-T8, cat. 558207), CD8 APC-H7 (BD, clone SK1, cat. 641400), CD14 PE-Cy7 (BD, clone M5E2, cat. 557742), CD14 APC-H7 (BD, clone MφP9, cat. 560270), CD16 PE (BD, 560995, clone 3G8), CD20 PE-Cy7(BD, clone L27, cat. 335793), CD25-APC (eBioscience (San Diego, *CA*), clone BC96, cat. 17-0259-42), CD28 PerCP-Cy5.5 (BD, clone L293, cat. 337181), CD56 PE (BD, clone B159, cat. 555516), CD69 APC (BD, clone L78, cat. 340560), biotin-conjugated CD95, (BD, clone DX2, cat. 555672), Mattapi integrin APC (BD, clone FIB504, cat. 551082).

Preparation of lymph node cells

Inguinal lymph nodes were surgically removed 14 days after infection from the two anaesthetised SIVmac251-infected macaques and stored on ice. They were cut into approximate 2 mm pieces with scissors and carefully ground into a slurry using a 5 ml syringe plunger (Terumo, Somerset, NJ) and washed through a 70 μm "Cell Strainer" filter (BD) with RPMI media (Gibco, Invitrogen). Cell numbers were determined using an ACT DIFF Coulter Counter® (Beckman Coulter, Brea, *CA*).

Preparation and storage of peripheral blood mononuclear cells (PBMCs)

Fresh blood, stored in heparinised or EDTA-coated vials was carefully layered over 95% Ficoll-Paque PLUS™ (GE Healthcare, Buckinghamshire, England)/5% water (V/V) and centrifuged at 1000 g for 25 min at room temperature. The interface was recovered using a transfer pipette and washed with RPMI media and centrifuged at 500 g for 5 min at room temperature. Cell counts were performed using an ACT DIFF Coulter Counter®. PBMCs were resuspended in a solution of 90% FCS (Bovogen Biologicals, East Keilor, Victoria, Australia)/10% (v/v) dimethylsulphoxide (Sigma-Aldrich St. Louis, MO) at a concentration of 5×10^6 cells/ml and frozen in a "Mr Frosty" freezing container (ThermoFisher Scientific) at −80 °C before long-term storage in liquid nitrogen.

Cell staining for flow cytometry

Fresh, heparinised, whole blood (200 μl) or inguinal lymph node cell preparations were surface-stained for CD3, CD8 and CD4 at room temperature for 20 min. For selected experiments antibodies T cell memory markers (CD28 and CD95), activation markers (CD25 and CD69), B cells (CD20), monocytes (CD14) or HLA-ABC, and the mucosal homing marker $\beta7$ and were also included. To detect biotinylated CD95 staining, a streptavidin-PE conjugate was used at 25 ng/ml for 30 min at room temperature. Red blood cells were lysed using 1 × FACs™ Lysing Solution (BD) or OptiLyse® C (Beckman Coulter) according to the manufacturer's guidelines and white blood cells were then permeabilised using 1 × FACs™ Permeabilising Solution (BD). Permeabilised cells were incubated with 0.125 μg in 50 μl anti-p27-FITC, at room temperature for 30 min before washing with 2 ml PBS and fixing with 1% paraformaldehyde (Polysciences Inc., Warrington, PA) or Stabilizing Fixative (BD).

Frozen PBMCs (1 ml at 5×10^6 cells/ml) were rapidly thawed in a 37 °C water-bath then incubated for 10 min in 3 ml RPMI/10%FCS 66 U/ml DNase in a 37 °C water-bath, followed by washing in the same media. PBMCs were incubated with LIVE/DEAD

fixable Aqua Dead Cell Stain (Molecular probes, Invitrogen) for 30 min followed by a wash in 1 × PBS/0.5% (w/v) BSA/2 mM EDTA. PBMCs were then surface-stained for CD2, CD3, CD4, CD5, CD8, CD20 and a combination of CD16a and CD56 which together mark NK cells in macaques, as well as some CD16 positive granulocytes and CD56 positive monocytes (Reeves et al., 2010). These cells were then fixed in 1 × PBS/1% (v/v) formaldehyde for 10 min, washed in 2 ml PBS then subject to permeabilisation as described above. Permeabilised cells were incubated with 0.0416 μg of anti-p27-FITC for 30 min at room temperature followed by washing and fixing as described above.

Flow cytometry

Acquisition was performed on a FACSCanto II or LSRII flow cytometer (BD) according to the manufacturer's instructions and data were analysed using FlowJo Version 9.2 (TreeStar, Ashland, USA). Flow cytometer compensation was set up using the auto-compensation function using calibrate™ beads (BD) for FITC, PE and APC and CompBead PLUS anti-rat Ig κ beads (BD) stained singly with individual antibodies used in the experimental samples. Mononuclear cells were gated according to scatter properties and aggregates excluded. CD8 negative cells that were CD3-positive, CD3-low and CD3-negative were then examined for the presence of intracellular p27 and surface CD4. T cells were further identified by their expression of CD2 and CD5, monocytes by CD14, B cells by CD20, NK cells by both CD16 and CD56, naïve, central or effector memory T cells using CD28 and CD95, activated cells by CD25 and CD69, and T-cells expression the mucosal homing integrin $\alpha 4\beta 7$ were also detected.

Determination of viral load

SIV viral load was determined as previously described, with some modifications (Leutenegger et al., 2001). Fresh, EDTA-treated whole blood, was centrifuged at 950 g for 12 min at room temperature. Plasma was recovered from the top layer and stored at −80 °C. RNA was isolated from 140 or 280 μl plasma using a QIAamp Viral RNA kit (Qiagen, Hilden, Germany) according to the manufacturer's instructions. SIV viral load was determined by qPCR by a Superscript® III RT-PCR reaction (Invitrogen) using TaqMan® Universal PCR Mastermix (Applied Biosystems Inc, Foster City, *CA*) according to the manufacturers' instructions. An 81 bp product in the SIV *GAG* gene was amplified using the primers 5′-CAACAGGCT-CAGAAAA-3′(forward) and 5′-TTTTCTGAGCCTGTTG-3′ (reverse) and detected using the Taqman® probe 5′-ATAATACTGTCTGCGT-CATCTGGTG-3′ using a Mastercycler® ep Realplex^4 instrument (Eppendorf, Hamburg, Germany). Sample viral load was determined using a standard curve made from *in vitro*-transcribed SIV RNA. To make the standards, a 670nt *GAG* RNA product was *in vitro*-transcribed using a MEGAscript® T7 kit (Ambion, Inc, Austin, TX), treated with TURBO™ DNase (Ambion) and RNA of the correct size was quantified using an Agilent 2100 Bioanalyser (Agilent, Santa Clara, *CA*). Negative controls were included where the reverse transcriptase enzyme was omitted.

Statistical analyses

Statistical analyses were performed using SPSS version 18 software (IBM, Armonk, NY, USA). Data in Fig. 1D and E were $\log_{10}$-transformation prior to analysis by one-way ANOVA in conjunction with Tukey's post-hoc test. After transformation, the data did not pass Levene's test for equal variances but were close to $p=0.05$, therefore the α level for one-way ANOVAs was set at 0.01. Data in Fig. 2A were analysed by a Friedman test, followed by Wilcoxon Signed Rank tests. These non-parametric tests were necessary as many of the values were 0. A Bonferroni adjustment was used to set a new α level of 0.017 for these analyses. Data in Fig. 6B were analysed by a Kruskal Wallis test.

Acknowledgments

We thank Nancy Wilson, Sinthujuan Jegaskanda, Pradeep Sidana, Caroline Fernandez, Megan Schepers, Camden Lo and John Zaunders for generous assistance, reagents and advice. This work was supported NHMRC grants and fellowships (1013221, 1011578 and 510448).

References

Aiken, C., Konner, J., Landau, N.R., Lenburg, M.E., Trono, D., 1994. Nef induces CD4 endocytosis: requirement for a critical dileucine motif in the membrane-proximal CD4 cytoplasmic domain. Cell 76, 853–864.

Arthos, J., Cicala, C., Martinelli, E., Macleod, K., Van Ryk, D., Wei, D., Xiao, Z., Veenstra, T.D., Conrad, T.P., Lempicki, R.A., McLaughlin, S., Pascuccio, M., Gopaul, R., McNally, J., Cruz, C.C., Censoplano, N., Chung, E., Reitano, K.N., Kottilil, S., Goode, D.J., Fauci, A.S., 2008. HIV-1 envelope protein binds to and signals through integrin alpha4beta7, the gut mucosal homing receptor for peripheral T cells. Nat. Immunol. 9, 301–309.

Bell, I., Schaefer, T.M., Trible, R.P., Amedee, A., Reinhart, T.A., 2001. Down-modulation of the costimulatory molecule, CD28, is a conserved activity of multiple SIV Nefs and is dependent on histidine 196 of Nef. Virology 283, 148–158.

Bernstein, H.B., Wang, G., Plasterer, M.C., Zack, J.A., Ramasastry, P., Mumenthaler, S.M., Kitchen, C.M., 2009. CD4+ NK cells can be productively infected with HIV, leading to downregulation of CD4 expression and changes in function. Virology 387, 59–66.

Brenchley, J.M., Hill, B.J., Ambrozak, D.R., Price, D.A., Guenaga, F.J., Casazza, J.P., Kuruppu, J., Yazdani, J., Migueles, S.A., Connors, M., Roederer, M., Douek, D.C., Koup, R.A., 2004. T-cell subsets that harbor human immunodeficiency virus (HIV) *in vivo*: implications for HIV pathogenesis. J. Virol. 78, 1160–1168.

Cayota, A., Vuillier, F., Scott-Algara, D., Feuillie, V., Dighiero, G., 1993. Differential requirements for HIV-1 replication in naive and memory CD4 T cells from asymptomatic HIV-1 seropositive carriers and AIDS patients. Clin. Exp. Immunol. 91, 241–248.

Centlivre, M., Legrand, N., Steingrover, R., van der Sluis, R., Grijsen, M.L., Bakker, M., Jurriaans, S., Berkhout, B., Paxton, W.A., Prins, J.M., Pollakis, G., 2011. Altered dynamics and differential infection profiles of lymphoid and myeloid cell subsets during acute and chronic HIV-1 infection. J. Leukoc. Biol. 89, 785–795.

Chen, B.K., Gandhi, R.T., Baltimore, D., 1996. CD4 down-modulation during infection of human T cells with human immunodeficiency virus type 1 involves independent activities of vpu, env, and nef. J. Virol. 70, 6044–6053.

Cicala, C., Martinelli, E., McNally, J.P., Goode, D.J., Gopaul, R., Hiatt, J., Jelicic, K., Kottilil, S., Macleod, K., O'Shea, A., Patel, N., Van Ryk, D., Wei, D., Pascuccio, M., Yi, L., McKinnon, L., Izulla, P., Kimani, J., Kaul, R., Fauci, A.S., Arthos, J., 2009. The integrin alpha4beta7 forms a complex with cell-surface CD4 and defines a T-cell subset that is highly susceptible to infection by HIV-1. Proc. Natl. Acad. Sci. USA 106, 20877–20882.

Craig, H.M., Pandori, M.W., Guatelli, J.C., 1998. Interaction of HIV-1 Nef with the cellular dileucine-based sorting pathway is required for CD4 down-regulation and optimal viral infectivity. Proc. Natl. Acad. Sci. USA 95, 11229–11234.

Czerkinsky, C., Holmgren, J., 1994. Exploration of mucosal immunity in humans: relevance to vaccine development. Cell. Mol. Biol. (Noisy-le-grand) 40 (Suppl 1), 37–44.

Das, S.R., Jameel, S., 2005. Biology of the HIV Nef protein. Indian J. Med. Res. 121, 315–332.

Deacon, N.J., Tsykin, A., Solomon, A., Smith, K., Ludford-Menting, M., Hooker, D.J., McPhee, D.A., Greenway, A.L., Ellett, A., Chatfield, C., Lawson, V.A., Crowe, S., Maerz, A., Sonza, S., Learmont, J., Sullivan, J.S., Cunningham, A., Dwyer, D., Dowton, D., Mills, J., 1995. Genomic structure of an attenuated quasi species of HIV-1 from a blood transfusion donor and recipients. Science 270, 988–991.

Flamand, L., Crowley, R.W., Lusso, P., Colombini-Hatch, S., Margolis, D.M., Gallo, R.C., 1998. Activation of CD8+ T lymphocytes through the T cell receptor turns on CD4 gene expression: implications for HIV pathogenesis. Proc. Natl. Acad. Sci. USA 95, 3111–3116.

Foster, J.L., Garcia, J.V., 2008. HIV-1 Nef: at the crossroads. Retrovirology 5, 84.

Friedrich, T.C., Piaskowski, S.M., Leon, E.J., Furlott, J.R., Maness, N.J., Weisgrau, K.L., Mac Nair, C.E., Weiler, A.M., Loffredo, J.T., Reynolds, M.R., Williams, K.Y., Klimentidis, Y.C., Wilson, N.A., Allison, D.B., Rakasz, E.G., 2010. High viremia is associated with high levels of *in vivo* major histocompatibility complex class I downregulation in rhesus macaques infected with simian immunodeficiency virus SIVmac239. J. Virol. 84, 5443–5447.

Greenberg, M.E., Bronson, S., Lock, M., Neumann, M., Pavlakis, G.N., Skowronski, J., 1997. Co-localization of HIV-1 Nef with the AP-2 adaptor protein complex correlates with Nef-induced CD4 down-regulation. EMBO J. 16, 6964–6976.

Heeregrave, E.J., Geels, M.J., Brenchley, J.M., Baan, E., Ambrozak, D.R., van der Sluis, R.M., Bennemeer, R., Douek, D.C., Goudsmit, J., Pollakis, G., Koup, R.A., Paxton, W.A., 2009. Lack of *in vivo* compartmentalization among HIV-1 infected naive and memory CD4+ T cell subsets. Virology 393, 24–32.

Huete, J.M., Chatis, P.A., Schmitz, J.E., Kuroda, M.J., Letvin, N.L., Reimann, K.A., 2001. Detection of viral RNA in CD4(−)CD8(−) and CD4(−)CD8(+) lymphocytes *in vivo* in rhesus monkeys infected with simian immunodeficiency virus of macaques. AIDS Res. Hum. Retroviruses 17, 349–360.

Iafrate, A.J., Carl, S., Bronson, S., Stahl-Hennig, C., Swigut, T., Skowronski, J., Kirchhoff, F., 2000. Disrupting surfaces of nef required for downregulation of CD4 and for enhancement of virion infectivity attenuates simian immunodeficiency virus replication *in vivo*. J. Virol. 74, 9836–9844.

Kader, M., Wang, X., Piatak, M., Lifson, J., Roederer, M., Veazey, R., Mattapallil, J.J., 2009. Alpha4(+)beta7(hi)CD4(+) memory T cells harbor most Th-17 cells and are preferentially infected during acute SIV infection. Mucosal Immunol. 2, 439–449.

Kent, S.J., Dale, C.J., Preiss, S., Mills, J., Campagna, D., Purcell, D.F., 2001. Vaccination with attenuated simian immunodeficiency virus by DNA inoculation. J. Virol. 75, 11930–11934.

Kent, S.J., Dale, C.J., Ranasinghe, C., Stratov, I., De Rose, R., Chea, S., Montefiori, D.C., Thomson, S., Ramshaw, I.A., Coupar, B.E., Boyle, D.B., Law, M., Wilson, K.M., Ramsay, A.J., 2005. Mucosally-administered human-simian immunodeficiency virus DNA and fowlpoxvirus-based recombinant vaccines reduce acute phase viral replication in macaques following vaginal challenge with CCR5-tropic SHIVSF162P3. Vaccine 23, 5009–5021.

Kilshaw, P.J., Murant, S.J., 1991. Expression and regulation of beta 7(beta p) integrins on mouse lymphocytes: relevance to the mucosal immune system. Eur. J. Immunol. 21, 2591–2597.

Klatt, N.R., Canary, L.A., Vanderford, T.H., Vinton, C.L., Engram, J.C., Dunham, R.M., Cronise, H.E., Swerczek, J.M., Lafont, B.A., Picker, L.J., Silvestri, G., Brenchley, J.M., 2011. Dynamics of SIVmac239 infection in Pigtail Macaques. J. Virol.

Letvin, N.L., Mascola, J.R., Sun, Y., Gorgone, D.A., Buzby, A.P., Xu, L., Yang, Z.Y., Chakrabarti, B., Rao, S.S., Schmitz, J.E., Montefiori, D.C., Barker, B.R., Bookstein, F.L., Nabel, G.J., 2006. Preserved CD4+ central memory T cells and survival in vaccinated SIV-challenged monkeys. Science 312, 1530–1533.

Leutenegger, C.M., Higgins, J., Matthews, T.B., Tarantal, A.F., Luciw, P.A., Pedersen, N.C., North, T.W., 2001. Real-time TaqMan PCR as a specific and more sensitive alternative to the branched-chain DNA assay for quantitation of simian immunodeficiency virus RNA. AIDS Res. Hum. Retrov. 17, 243–251.

Levesque, K., Finzi, A., Binette, J., Cohen, E.A., 2004. Role of CD4 receptor down-regulation during HIV-1 infection. Curr. HIV Res. 2, 51–59.

Li, Q., Duan, L., Estes, J.D., Ma, Z.M., Rourke, T., Wang, Y., Reilly, C., Carlis, J., Miller, C.J., Haase, A.T., 2005. Peak SIV replication in resting memory CD4+ T cells depletes gut lamina propria CD4+ T cells. Nature 434, 1148–1152.

Livingstone, W.J., Moore, M., Innes, D., Bell, J.E., Simmonds, P., 1996. Frequent infection of peripheral blood CD8-positive T-lymphocytes with HIV-1. Edinburgh Heterosexual Transmission Study Group. Lancet 348, 649–654.

Loh, L., Petravic, J., Batten, C.J., Davenport, M.P., Kent, S.J., 2008. Vaccination and timing influence SIV immune escape viral dynamics *in vivo*. PLoS Pathog. 4, e12.

Marodon, G., Warren, D., Filomio, M.C., Posnett, D.N., 1999. Productive infection of double-negative T cells with HIV *in vivo*. Proc. Natl. Acad. Sci. USA 96, 11958–11963.

Martin, R.A., Nayak, D.P., 1996. Membrane anchorage of gp160 is necessary and sufficient to prevent CD4 transport to the cell surface. Virology 220, 473–479.

Mattapallil, J.J., Douek, D.C., Hill, B., Nishimura, Y., Martin, M., Roederer, M., 2005. Massive infection and loss of memory CD4+ T cells in multiple tissues during acute SIV infection. Nature 434, 1093–1097.

McDougal, J.S., Mawle, A., Cort, S.P., Nicholson, J.K., Cross, G.D., Scheppler-Campbell, J.A., Hicks, D., Sligh, J., 1985. Cellular tropism of the human retrovirus HTLV-III/LAV. I. Role of T cell activation and expression of the T4 antigen. J. Immunol. 135, 3151–3162.

Meditz, A.L., Haas, M.K., Folkvord, J.M., Melander, K., Young, R., McCarter, M., Mawhinney, S., Campbell, T.B., Lie, Y., Coakley, E., Levy, D.N., Connick, E., 2011. HLA-DR+CD38+CD4+ T lymphocytes have elevated CCR5 expression and produce the majority of R5-tropic HIV-1 RNA *in vivo*. J. Virol..

Mercure, L., Phaneuf, D., Wainberg, M.A., 1993. Detection of unintegrated human immunodeficiency virus type 1 DNA in persistently infected CD8+ cells. J. Gen. Virol. 74 (Pt 10), 2077–2083.

Nabel, G., Baltimore, D., 1987. An inducible transcription factor activates expression of human immunodeficiency virus in T cells. Nature 326, 711–713.

Pahar, B., Lackner, A.A., Veazey, R.S., 2006. Intestinal double-positive CD4+CD8+ T cells are highly activated memory cells with an increased capacity to produce cytokines. Eur. J. Immunol. 36, 583–592.

Pitcher, C.J., Hagen, S.I., Walker, J.M., Lum, R., Mitchell, B.L., Maino, V.C., Axthelm, M.K., Picker, L.J., 2002. Development and homeostasis of T cell memory in rhesus macaque. J. Immunol. 168, 29–43.

Reeves, R.K., Evans, T.I., Gillis, J., Johnson, R.P., 2010. Simian immunodeficiency virus infection induces expansion of alpha4beta7+ and cytotoxic CD56+ NK cells. J. Virol. 84, 8959–8963.

Reynolds, M.R., Piaskowski, S.M., Weisgrau, K.L., Weiler, A.M., Friedrich, T.C., Rakasz, E.G., 2010. Ex vivo analysis of SIV-infected cells by flow cytometry. Cytometry A 77, 1059–1066.

Sanfridson, A., Cullen, B.R., Doyle, C., 1994. The simian immunodeficiency virus Nef protein promotes degradation of CD4 in human T cells. J. Biol. Chem. 269, 3917–3920.

Schindler, M., Munch, J., Kutsch, O., Li, H., Santiago, M.L., Bibollet-Ruche, F., Muller-Trutwin, M.C., Novembre, F.J., Peeters, M., Courgnaud, V., Bailes, E., Roques, P., Sodora, D.L., Silvestri, G., Sharp, P.M., Hahn, B.H., Kirchhoff, F., 2006. Nef-mediated suppression of T cell activation was lost in a lentiviral lineage that gave rise to HIV-1. Cell 125, 1055–1067.

Schindler, M., Schmokel, J., Spect, A., Li, H., Munch, J., Khalid, M., Sodora, D.L., Hahn, B.H., Silvestri, G., Kirchhoff, F., 2008. Inefficient Nef-mediated down-modulation of CD3 and MHC-I correlates with loss of CD4+ T cells in natural SIV infection. PLOS pathogens 4, e1000107.

Schnittman, S.M., Lane, H.C., Greenhouse, J., Justement, J.S., Baseler, M., Fauci, A.S., 1990. Preferential infection of CD4+ memory T cells by human immunodeficiency virus type 1: evidence for a role in the selective T-cell functional defects observed in infected individuals. Proc. Natl. Acad. Sci. USA 87, 6058–6062.

Schnittman, S.M., Psallidopoulos, M.C., Lane, H.C., Thompson, L., Baseler, M., Massari, F., Fox, C.H., Salzman, N.P., Fauci, A.S., 1989. The reservoir for HIV-1 in human peripheral blood is a T cell that maintains expression of CD4. Science 245, 305–308.

Schwartz, O., Marechal, V., Le Gall, S., Lemonnier, F., Heard, J.M., 1996. Endocytosis of major histocompatibility complex class I molecules is induced by the HIV-1 Nef protein. Nat. Med. 2, 338–342.

Swigut, T., Shohdy, N., Skowronski, J., 2001. Mechanism for down-regulation of CD28 by Nef. EMBO J. 20, 1593–1604.

Willerford, D.M., Gale Jr., M.J., Benveniste, R.E., Clark, E.A., Gallatin, W.M., 1990. Simian immunodeficiency virus is restricted to a subset of blood CD4+ lymphocytes that includes memory cells. J. Immunol. 144, 3779–3783.